Search for Heavy Sterile Neutrinos in Trileptons at the LHC

Claudio O. Dib,[1,*] C. S. Kim,[2,†] and Kechen Wang[3,4,‡]

[1] *CCTVal and Department of Physics, Universidad Técnica Federico Santa María, Valparaíso, Chile*
[2] *Department of Physics and IPAP, Yonsei University, Seoul 120-749, Korea*
[3] *DESY, Notkestrae 85, D-22607 Hamburg, Germany*
[4] *Center for Future High Energy Physics, Institute of High Energy Physics, Chinese Academy of Sciences, Beijing, 100049, China*

(Dated: March 20, 2017)

We present a search strategy for both Dirac and Majorana sterile neutrinos from the purely leptonic decays of $W^\pm \to e^\pm e^\pm \mu^\mp \nu$ and $\mu^\pm \mu^\pm e^\mp \nu$ at the 14 TeV LHC. The discovery and exclusion limits for sterile neutrinos are shown using both the Cut-and-Count (CC) and Multi-Variate Analysis (MVA) methods. We also discriminate between Dirac and Majorana sterile neutrinos by exploiting a set of kinematic observables which differ between the Dirac and Majorana cases. We find that the MVA method, compared to the more common CC method, can greatly enhance the discovery and discrimination limits. Two benchmark points with sterile neutrino mass $m_N = 20$ GeV and 50 GeV are tested. For an integrated luminosity of 3000 fb^{-1}, sterile neutrinos can be found with 5σ significance if heavy-to-light neutrino mixings $|U_{Ne}|^2 \sim |U_{N\mu}|^2 \sim 10^{-6}$, while Majorana vs. Dirac discrimination can be reached if at least one of the mixings is of order 10^{-5}.

PACS numbers: 14.60.St, 13.35.Hb, 11.30.Hv.

Introduction The evidence of small but non zero neutrino masses [1] is currently an outstanding path beyond the Standard Model of particle physics. Most explanations are based on the existence of extra heavy particles. In particular, seesaw models involve extra heavy neutrinos that are sterile under electroweak interactions, but which mix with the Standard leptons [2]. Moreover, in most scenarios they are Majorana fermions [3]. The existence of heavy neutrinos and the discrimination between Dirac and Majorana is thus a crucial piece of information that experiments must reveal. The Majorana nature of neutrinos is searched in neutrinoless double beta decays [4], but so far no experimental evidence has been found [5]. The Large Hadron Collider (LHC) also offers the possibility to search for same-sign dilepton plus dijet events, $\ell^\pm \ell^\pm jj$, produced if there are heavy Majorana neutrinos (henceforth called N) in the intermediate state with masses above M_W [6]. Instead, for masses below M_W, the jets are lost in the background and thus trilepton events $\ell^\pm \ell^\pm \ell'^\mp \nu$ provide clearer signals for a heavy N [7], where ℓ and ℓ' denote leptons with different flavors. The choice of having no Opposite-Sign Same-Flavor (no-OSSF) lepton pairs helps eliminate a serious SM background $\gamma^*/Z \to \ell^+\ell^-$ [8]. Now, if N is Majorana, the trilepton will contain a Lepton Number Conserving (LNC) channel $W^+ \to e^+e^+\mu^-\nu_e$ as well as a Lepton Number Violating (LNV) channel $W^+ \to e^+e^+\mu^-\bar{\nu}_\mu$, while if it is of Dirac type, only the LNC channel will appear. However, since the final neutrino escapes the detection, the observed final state is just $e^\pm e^\pm \mu^\mp$ or $\mu^\pm \mu^\pm e^\mp$ plus missing energy. Hence it is not a simple task to distinguish a Majorana vs. a Dirac N. In our previous work [9], we studied these trilepton events to discover heavy neutrinos and discriminate between Dirac and Majorana using differences in their energy distributions. In our consecutive work [10], we presented a simpler method for this discrimination by comparing the full rates of $e^\pm e^\pm \mu^\mp$ and $\mu^\pm \mu^\pm e^\mp$. However, this discrimination based on full rates only works if the mixing parameters U_{Ne} and $U_{N\mu}$ are considerably different from each other (See Table 1).

Discovery Limit: In this letter, we present a strategy to discover heavy sterile neutrinos N with $m_N < M_W$, and discriminate between their Dirac vs. Majorana character, using trilepton events at the 14 TeV LHC, applying both a Cut-and-Count (CC) and a Multi-Variate Analysis (MVA) methods. Our strategy is most complete in the sense that uses all details of each event, including spectra and angular distributions.

We consider the process $W^\pm \to l_W^\pm l_N^\pm l'^\mp_N \nu$ (Fig. 1), where l and l' are different leptons, either e or μ (i.e. $e^\pm e^\pm \mu^\mp \nu$ and $\mu^\pm \mu^\pm e^\mp \nu$), and ν is a SM neutrino or antineutrino. For convenience, we introduce two parameters: a *normalization* factor s and a *disparity* factor r:

$$s \equiv 2 \times 10^6 \, \frac{|U_{Ne} U_{N\mu}|^2}{|U_{Ne}|^2 + |U_{N\mu}|^2}, \quad r \equiv \frac{|U_{Ne}|^2}{|U_{N\mu}|^2}. \qquad (1)$$

Conversely, the heavy-to-light mixing elements $|U_{Ne}|^2$ and $|U_{N\mu}|^2$ can be expressed in terms of r and s as:

$$|U_{Ne}|^2 = \frac{s\,(1+r)}{2 \times 10^6}, \quad |U_{N\mu}|^2 = \frac{s\,(1+\frac{1}{r})}{2 \times 10^6}. \qquad (2)$$

For our study we choose two benchmark points: $m_N =$ 20 and 50 GeV, with $r = s = 1$ (i.e., $|U_{Ne}|^2 = |U_{N\mu}|^2 =$

* claudio.dib@usm.cl
† cskim@yonsei.ac.kr
‡ kechen.wang@desy.de

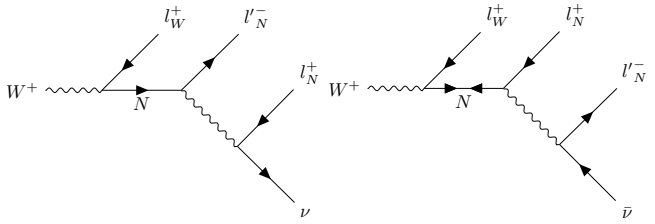

FIG. 1. The LNC process $W^+ \to l_W^+ l'^-_N l_N^+ \nu$, mediated by a heavy sterile neutrino of Majorana or Dirac type (left); and the LNV process $W^+ \to l_W^+ l_N^+ l'^-_N \bar{\nu}$, mediated by a heavy sterile neutrino of Majorana type (right);

10^{-6}). The production rates of the different trilepton modes are proportional to the scale factors shown in Table I.

	Dirac	Majorana
$e^\pm e^\pm \mu^\mp$	s	$s\,(1+r)$
$\mu^\pm \mu^\pm e^\mp$	s	$s\,(1+1/r)$

TABLE I. Scale factors for the production rates of the trilepton final states. See Eq. (1) for the definitions of s and r.

Let us first describe our strategy to discover or set exclusion limits for Dirac and Majorana sterile neutrinos using trileptons at the LHC. We first select trilepton events $l^\pm l^\pm l'^\mp$ with no-OSSF lepton pairs. Then we apply basic cuts for leptons and jets: $p_{T,l} \geq 10$ GeV and $|\eta_l| \leq 2.5$; $p_{T,j} \geq 20$ GeV and $|\eta_j| \leq 5.0$, and veto the b-jets in order to suppress the $t\bar{t}$ background. Now, in order to select within the pair $l^\pm l^\pm$ the lepton that comes from the N decay, we construct the χ^2 function

$$\chi^2 = (\mathcal{M}_W - m_W)^2/\sigma_W^2 + (\mathcal{M}_N - m_N)^2/\sigma_N^2, \qquad (3)$$

where $m_W = 80.5$ GeV and m_N is the assumed mass for N (20 or 50 GeV in our benchmarks), while $\mathcal{M}_W$ and $\mathcal{M}_N$ are the reconstructed invariant masses of $l^\pm l^\pm l'^\mp \nu$ and $l^\pm l'^\mp \nu$, respectively; σ_W and σ_N are the widths of the reconstructed mass distributions, which we take to be 5% of their respective m_W and m_N, for simplicity. When calculating the reconstructed mass M_W and M_N, the final neutrino transverse momentum $\mathbf{p}_{T,\nu}$ is assumed to be the missing transverse momentum, while the neutrino longitudinal momentum $p_{z,\nu}$ and the correct lepton $l^\pm$ from the N decay are determined by minimizing the χ^2 of Eq. (3). A better identification of the correct lepton can be achieved if the production and decay vertices of N are spatially displaced in the detector [11, 12]. However, this would be perceptible only if $m_N \lesssim 15$ GeV.

Then a MVA is performed to exploit the useful observables and maximally reduce the SM background. We use the *Boosted Decision Trees* (BDT) method in the TMVA package [13] and input the following kinematical observables for training and test processes: (i) the missing energy $\not{E}_T$; (ii) the scalar sum of p_T of all jets H_T; (iii) the transverse mass of the missing energy plus lepton(s) $M_T(\not{E}_T, l_W l_N l'_N)$, $M_T(\not{E}_T, l_N l'_N)$, $M_T(\not{E}_T, l_W l'_N)$, $M_T(\not{E}_T, l_W)$, $M_T(\not{E}_T, l_N)$, $M_T(\not{E}_T, l'_N)$; (iv) the azimuthal angle difference $\Delta\phi$ between the missing transverse momentum and lepton(s) $\Delta\phi(\not{E}_T, l_N l'_N)$, $\Delta\phi(\not{E}_T, l_W l'_N)$, $\Delta\phi(\not{E}_T, l_W)$, $\Delta\phi(\not{E}_T, l_N)$, $\Delta\phi(\not{E}_T, l'_N)$; (v) the invariant mass of the system of leptons $M(l_W l_N l'_N)$, $M(l_W l_N)$, $M(l_W l'_N)$, $M(l_N l'_N)$; and (vi) the azimuthal angle difference $\Delta\phi$ between two leptons $\Delta\phi(l_W, l'_N)$, $\Delta\phi(l_N, l'_N)$. For a Dirac (Majorana) N, the simulation data of the LNC (LNC + LNV) processes are inputs as the signal sample, while the total SM background data (γ^*/Z, WZ, and $t\bar{t}$ inclusively) are inputs as the background sample for the TMVA training and test processes. The details of our data simulation procedures are described in [10].

Fig. 2 shows the BDT response distributions for a Dirac N signal and total SM background, for our two benchmarks. The signal vs. background separation is better for $m_N = 20$ GeV than for $m_N = 50$ GeV, as the two curves have less overlap in Fig. 2 (left).

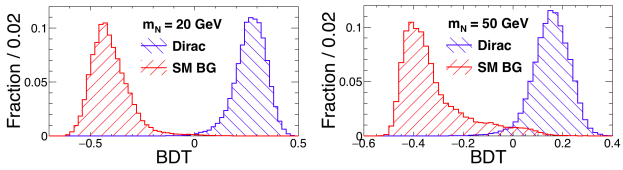

FIG. 2. Distributions of BDT response for Dirac signal (blue) with $m_N = 20$ (left) and 50 (right) GeV, and total SM backgrounds (red) including γ^*/Z+jets, WZ+jets and $t\bar{t}$.

In Table II, we show the number of events for both Dirac and Majorana signals with $m_N = 20$ GeV and the SM backgrounds at the 14 TeV LHC. The first two rows show the number of events after basic cuts and b-jets vetoes. The number of events using the CC method from Ref. [10] are shown in the third row. The numbers of events for Dirac (Majorana) sterile neutrinos using the BDT method are shown in the fourth (fifth) row. For a Dirac (Majorana) N, we get a statistical significance

$$SS = N_s/\sqrt{N_s + N_b} \qquad (4)$$

near 2.6 (5.8) for the CC method and near 6.6 (10.7) for the BDT method, where N_s and N_b are the number of signal events (either Dirac or Majorana) and SM background events, respectively. Similarly, Table III shows the numbers for $m_N = 50$ GeV. From Fig. 2, lower significances are expected for $m_N = 50$ GeV. Indeed, Table III shows SS near 2.3 (4.8) for the CC method and near 5.1 (9.0) for the BDT method.

Fig. 3 shows the discovery and exclusion curves for a Dirac N, for both the BDT and CC methods. By exploiting more useful kinematical observables and better optimization compared with the CC method, the BDT method can greatly enhance the discovery and exclusion limits. Due to the small number of signal events, the performance of the BDT method becomes close to that

Cuts	Dirac	Majorana	γ^*/Z	WZ	$t\bar{t}$	SS
Basic cuts	54.0	133.2	4220	2658	68588	
N(b-jets)=0	53.1	131.1	4063.0	2497.1	31953.5	
CC	44.2	110.9	209.8	25.3	16.9	2.6 (5.8)
BDT > 0.183	46.7	-	1.9	1.3	0.0	6.6
BDT > 0.171	-	120.7	5.1	1.7	0.8	10.7

TABLE II. Cut flow for signal and background processes with $m_N = 20$ GeV. Numbers of events correspond to an integrated luminosity of 3000 fb^{-1} at the 14 TeV LHC.

Cuts	Dirac	Majorana	γ^*/Z	WZ	$t\bar{t}$	SS
Basic cuts	108.4	228.8	4220	2658	68588	
N(b-jets)=0	106.7	225.2	4063.0	2497.1	31953.5	
CC	91.9	193.9	1283.1	120.7	48.9	2.3 (4.8)
BDT > 0.138	64.4	-	25.7	47.5	21.1	5.1
BDT > 0.138	-	143.2	31.0	52.8	27.0	9.0

TABLE III. Cut flow for signal and background processes with $m_N = 50$ GeV. Numbers of events correspond to an integrated luminosity of 3000 fb^{-1} at the 14 TeV LHC.

of CC method for small s values (see Table I). Using the BDT method, one can get significances $\geq 5.0\sigma\,(3.0\sigma)$ for $s \geq 0.55\,(0.25)$ at $m_N = 20$ GeV, or $s \geq 1.02\,(0.55)$ at $m_N = 50$ GeV.

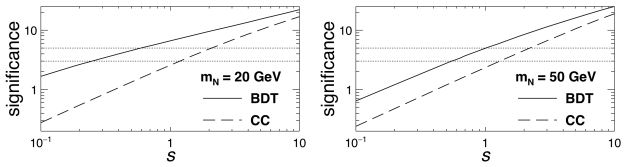

FIG. 3. Discovery and exclusion limits for Dirac sterile neutrinos with $m_N = 20$ (left) and 50 (right) GeV.

Fig. 4 shows the discovery and exclusion curves for a Majorana N, using both the BDT and CC methods. Here the rates depend on both s and r (see Table I), and so the observables at the LHC can be used to constrain both s and r. When $r = 1$, one can get a significance above $5.0\sigma\,(3.0\sigma)$ for $s \geq 0.24\,(0.11)$ at $m_N = 20$ GeV, or $s \geq 0.46\,(0.25)$ at $m_N = 50$ GeV. For a given s, the significance becomes larger when $r \neq 1$, due to the larger number of signal events. Using the BDT method, when $r \approx 10$, one can get significances $\geq 5.0\sigma\,(3.0\sigma)$ for $s \geq 0.08\,(0.03)$ at $m_N = 20$ GeV, or $s \geq 0.16\,(0.09)$ at $m_N = 50$ GeV.

Discrimination Limit: We now show that one can distinguish between a Dirac and Majorana N in the trilepton events, using the following distributions, which differ between the LNC and LNV processes: (i) the transverse mass of the system formed by the missing energy plus lepton(s) $M_T(\not{E}_T, l_N)$, $M_T(\not{E}_T, l'_N)$, and $M_T(\not{E}_T, l'_N l_W)$; and (ii) the azimuthal angle difference $\Delta\phi$ between the missing transverse momentum and lepton(s) $\Delta\phi(\not{E}_T, l_N)$, $\Delta\phi(\not{E}_T, l'_N)$, and $\Delta\phi(\not{E}_T, l'_N l_W)$.

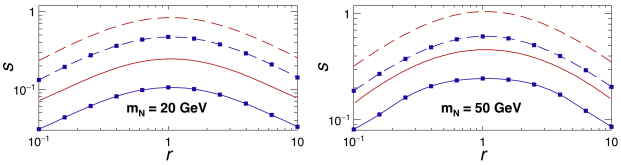

FIG. 4. Discovery and exclusion limits for Majorana sterile neutrinos with $m_N = 20$ (left) and 50 (right) GeV, where the blue curves marked with squares correspond to 3-σ limit, while the red curves correspond to 5-σ limit; solid lines for BDT method and dashed lines for CC method.

In order to exploit these differences, we must first reduce as much SM background as possible: after applying the basic cuts and vetoes, we perform the first BDT analysis and input the rest of the observables except those mentioned in the above paragraph to suppress the SM backgrounds. Simulated Majorana data are input as the signal sample, while the total SM background data are input as the background sample for TMVA training and testing processes. After the first BDT cut, the total number of events, for $M_N = 20$ GeV, including all four final states ($e^\pm e^\pm \mu^\mp$ and $\mu^\pm \mu^\pm e^\mp$) for the Dirac signals (the LNC rate only), Majorana signals (LNC + LNV rates) and SM backgrounds (γ^*/Z, $W^\pm Z$, and $t\bar{t}$ inclusively) are 48.5, 120.4 and 7.3, respectively.

Since s is a global scale a priori unknown, as a second step we adjust s for the Dirac hypothesis to match the number of events of the Majorana hypothesis, so that our simulation does not artificially distinguish the two scenarios simply by the rates. Just as in Ref. [10], the best matched value of $s_{\rm D}$ is found by minimizing:

$$\chi^2_H = -2 \min_s \left\{ \ln \left(\prod_i \text{Poiss}\left[N_i^{\rm expc}, N_i^{\rm obs}(s)\right] \right) \right\}, \quad (5)$$

where i indicates a particular trilepton final state, Poiss($N^{\rm expc}$, $N^{\rm obs}$) denotes the probability of observing $N^{\rm obs}$ events in Poisson statistics when the number of expected events is $N^{\rm expc}$. Here $N^{\rm expc}$ is the expected number of events for the Majorana hypothesis (LNC + LNV + SM background), while $N^{\rm obs}$ is the observed number of events for the Dirac hypothesis (LNC + SM background). The best matched $s_{\rm D}$ found in this way for the Dirac hypothesis gives the closest number of events to the Majorana case. For $m_N = 20$ GeV, we find $s_{\rm D} \sim 2.44$. After matching, the Dirac and Majorana hypotheses will have 125.6 and 127.6 events, respectively.

As a third step, we perform a second BDT analysis to distinguish Majorana from Dirac hypothesis by exploiting the differences in the distributions, mentioned above. Fig. 5 shows the distributions of two of these observables after basic cuts, b-jets veto and the first BDT cut. With an optimized second BDT cut of about 0.020, the Majorana case ends up with 46.1 events, while the Dirac hypothesis has 34.1 events. After defining the excess in the Majorana case from the Dirac hypothesis as the "signal" events N_s, and the number of events of the Dirac hypoth-

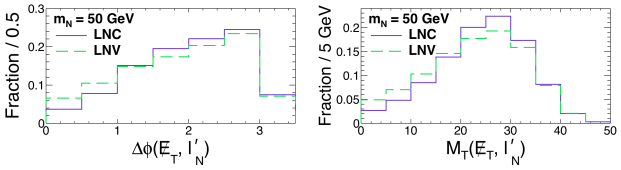

FIG. 5. Distributions for the benchmark point $m_N = 50$ GeV after applying the basic cuts, b-jets veto and the first BDT cut.

esis as the "background" events N_b, the significance for distinguishing Majorana from Dirac can be calculated as $s = N_s/\sqrt{N_s + N_b} = (46.1 - 34.1)/\sqrt{46.1} \approx 1.8$. This three-step method can be extended to the case where $r \neq 1$.

When $r \neq 1$, the number of events for different trilepton states will be quite different between Dirac and Majorana (see Table I), which helps in this discrimination and gives a higher significance. Fig. 6 shows the Confidence levels for distinguishing Majorana from Dirac after the above three-step method. When $r \approx 1$, one can have significances $\geq 5.0\sigma(3.0\sigma)$ for $s \geq 7.93(3.10)$ at $m_N = 20$ GeV, or $s \geq 11.44(5.47)$ at $m_N = 50$ GeV. As $r \approx 10$, the same significance is reached with lower $s \sim 0.25(0.10)$ at $m_N = 20$ GeV, or 0.72 (0.38) at $m_N = 50$ GeV.

Summary We present a complete method to discover or set exclusion limits for heavy sterile neutrinos with $m_N < M_W$, and discriminate their Dirac vs. Majorana nature, in trilepton final states at the 14 TeV LHC, using both Cut-and-Count (CC) and Multi-Variate Analysis (MVA). Expressing the mixings in terms of s and r [c.f. Eq. (1)], for an integrated luminosity of 3000 fb^{-1}, using the MVA method, a significance of 5.0 $(0.3)\sigma$ can be achieved when $s \geq 0.55(0.25)$ for a Dirac $m_N = 20$ GeV, or $s \geq 1.02(0.55)$ for $m_N = 50$ GeV. For Majorana sterile neutrinos, the same significances can be reached when $r \approx 10$, $s \geq 0.08(0.03)$ for $m_N = 20$ GeV, or $s \geq 0.16(0.09)$ for $m_N = 50$ GeV. Moreover, Majorana vs. Dirac can be distinguished with those significances when $r \approx 1$ and $s \geq 7.9(3.1)$ for $m_N = 20$ GeV, or $s \geq 11(5.8)$ for $m_N = 50$ GeV. As $r \approx 10$, the same significances are reached for $s \geq 0.25(0.10)$ for $m_N = 20$ GeV, or $s \geq 0.72(0.38)$ for $m_N = 50$ GeV.

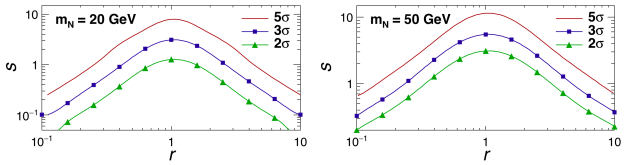

FIG. 6. Confidence levels of distinguishing between Dirac and Majorana neutrinos for $m_N = 20$ (left) and 50 (right) GeV.

ACKNOWLEDGMENTS

We thank Jue Zhang for his valuable help. K.W. was supported by the International Postdoctoral Exchange Fellowship Program (No.90 Document of OCPC, 2015); C.S.K. by the NRF grant funded by the Korean government of the MEST (No. 2016R1D1A1A02936965); and C.D. by Chile grants Fondecyt No. 1130617, Conicyt ACT 1406 and PIA/Basal FB0821.

[1] Y. Fukuda *et al.* [Super-Kamiokande Collaboration], Phys. Rev. Lett. **81**, 1562 (1998), hep-ex/9807003; Q. R. Ahmad *et al.* [SNO Collaboration], *ibid.* **89**, 011301 (2002), nucl-ex/0204008.

[2] J.W.F. Valle and J.C. Romao, *Neutrinos in high energy and astroparticle physics*, ISBN-13: 978-3527411979 (1st Edition, Wiley-VCH, Berlin, 2015).

[3] E. Majorana, Nuovo Cimento **14**, 171 (1937); G. Racah, *ibid.* **14**, 322 (1937).

[4] J. Engel and J. Menéndez, (2016), arXiv:1610.06548;

[5] H. V. Klapdor-Kleingrothaus *et al.*, Eur. Phys. J. A **12**, 147 (2001), hep-ph/0103062; A. M. Bakalyarov *et al.* [C03-06-23.1 Collaboration], Phys. Part. Nucl. Lett. **2**, 77 (2005) [Pisma Fiz. Elem. Chast. Atom. Yadra **2005**, 21 (2005)], hep-ex/0309016; H. V. Klapdor-Kleingrothaus and I. V. Krivosheina, Mod. Phys. Lett. A **21**, 1547 (2006); M. Agostini *et al.* [GERDA Collaboration], Phys. Rev. Lett. **111**, 122503 (2013), arXiv:1307.4720; A. Pocar [EXO-200 and nEXO Collaborations], Nucl. Part. Phys. Proc. **265-266**, 42 (2015); Y. Gando [KamLAND-Zen Collaboration], Nucl. Part. Phys. Proc. **273-275**, 1842 (2016); A. Gando *et al.* [KamLAND-Zen Collaboration], Phys. Rev. Lett. **117**, 082503 (2016); **117**, 109903 (2016), arXiv:1605.02889.

[6] G. Aad *et al.* [ATLAS Collaboration], JHEP **1507**, 162 (2015), arXiv:1506.06020; V. Khachatryan *et al.* [CMS Collaboration], Phys. Lett. B **748**, 144 (2015), arXiv:1501.05566.

[7] E. Izaguirre and B. Shuve, Phys. Rev. D **91**, 093010 (2015), arXiv:1504.02470.

[8] G. Cvetic, C.O. Dib and C.S. Kim, JHEP **1206**, 149 (2012), arXiv:1203.0573.

[9] C.O. Dib and C. S. Kim, Phys. Rev. D **92**, 093009 (2015), arXiv:1509.05981.

[10] C.O. Dib, C.S. Kim, K. Wang and J. Zhang, Phys. Rev. D **94**, 013005 (2016), arXiv:1605.01123.

[11] J. C. Helo, M. Hirsch and S. Kovalenko, Phys. Rev. D **89**, 073005 (2014); **93**, 099902(E) (2016), arXiv:1312.2900.

[12] C.O. Dib and C. S. Kim, Phys. Rev. D **89**, 077301 (2014), arXiv:1403.1985.

[13] P. Speckmayer, A. Hocker, J. Stelzer and H. Voss, J. Phys. Conf. Ser. **219**, 032057 (2010); A. Hocker *et al.*, PoS ACAT, 040 (2007), physics/0703039.